The Suspension Model
2003

EDC Library Ref. No. 1088

DISCLAIMER

B.9 Air Suspension Model

B.9.1 Introduction. This section is intended to explain the air suspension model of the Phase III simulation programs. There are a number of different air suspensions on the market. The model described here encompasses single and tandem axle designs using either four-bar- or trailing-arm-type linkages.

The air suspension model is conveniently divided into three parts:

1) the mechanical linkage system
2) the air spring
3) the air delivery system

These parts of the model will be dealt with successively in the next three sections. Section B.9.5 considers the interrelationships between the various parts of the model and Section B.9.6 discusses static considerations for the model.

B.9.2 The Mechanical Linkage System. The first linkage system to be modeled is the tandem four-bar type as illustrated in Figure 2.25. Dimensions relevant to the problem appear in the figure. Free-body diagrams of each link, showing all dynamic forces and moments acting on the links, appear in Figure B-29.

In the free bodies of Figure B-29, the dynamic tire normal forces (DN), viscous damping forces (FF), the air spring forces (FS), brake forces (FX), brake torques (TT), longitudinal decelerations (XDD), and their related D'Alembert forces (MS · XDD), are considered known "inputs" to the linkage, having been calculated earlier in other portions of the program. All other forces plus the vertical accelerations ($\ddot{Z}SP$) are unknown reactions to these forces.

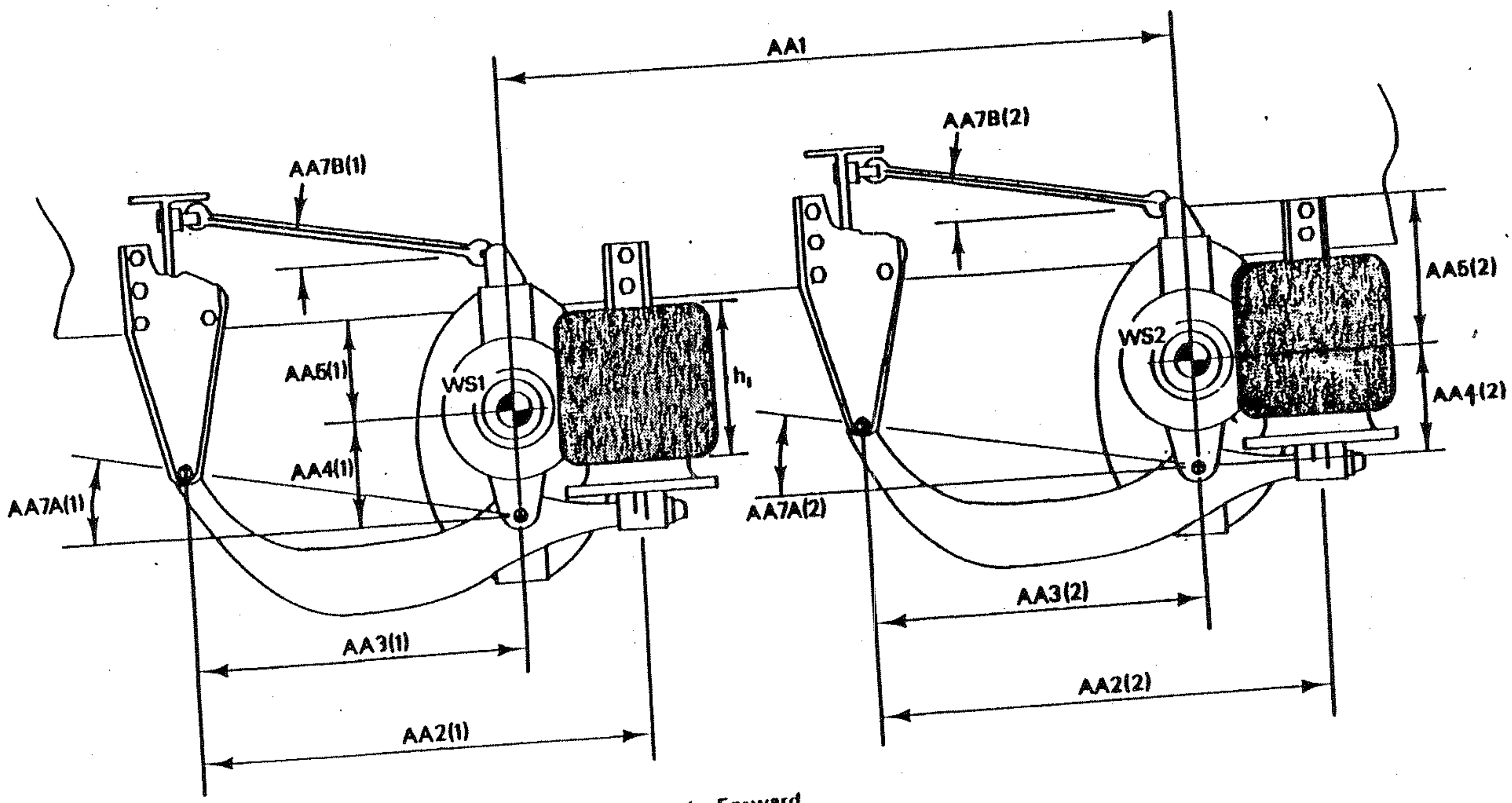

Figure 2.25. The air suspension model with four-bar linkage suspensions.

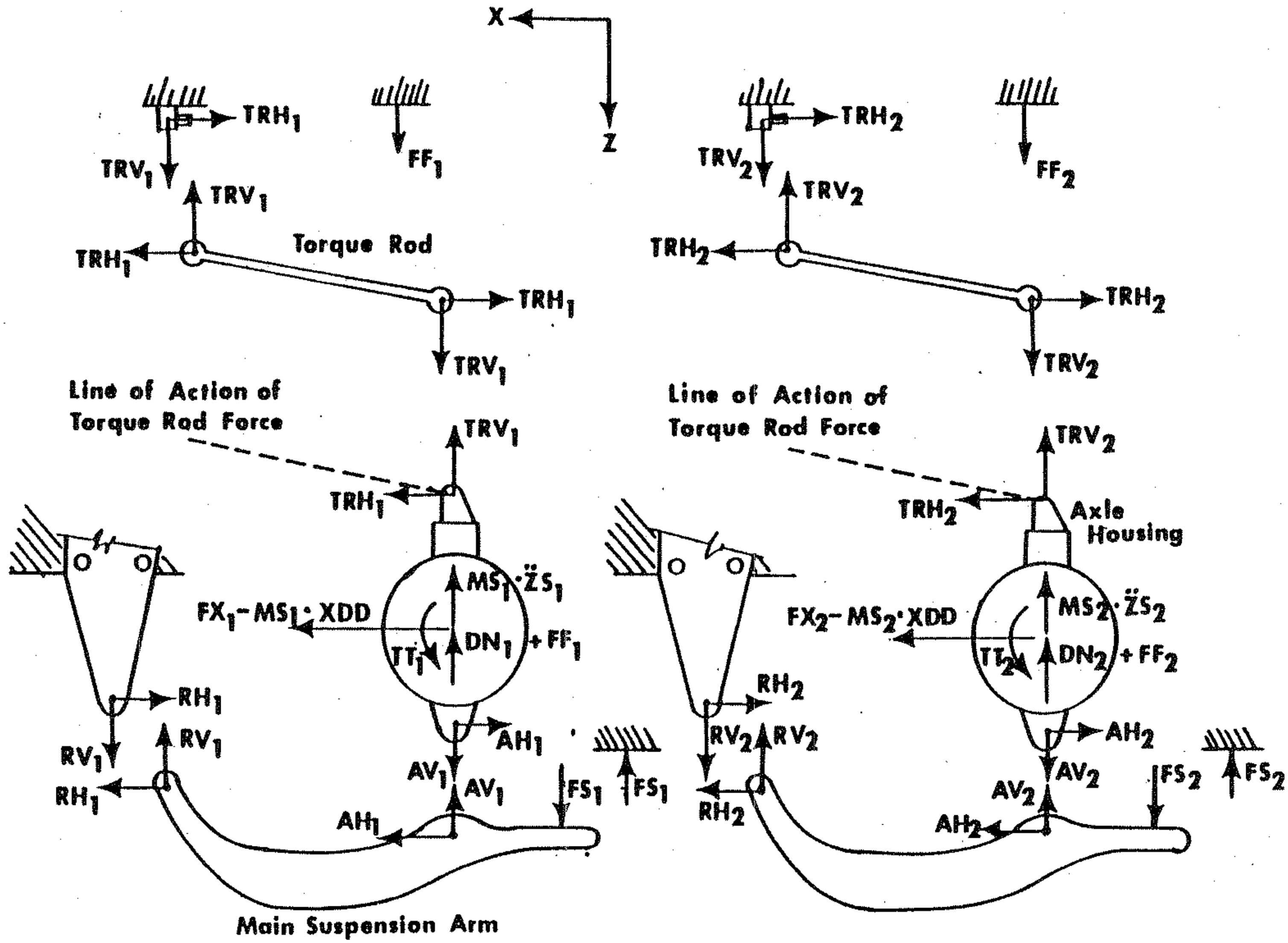

Figure B-29. Dynamic free-body diagram: tandem four-bar linkage air suspension

The assumptions on which the linkage model is based are:

1) Masses or moments of inertia are significant only with respect to vertical and longitudinal motion of the axle assembly.

2) The longitudinal accelerations of the unsprung masses are identical to that of sprung mass.

3) The mass center and axle center of each unsprung mass are coincident.

4) The pin connection between the main suspension arm and the axle housing lies directly below the axle center.

5) All pin connections are frictionless.

6) The air spring may transmit vertical force only.

7) Changes in geometry due to motions of the suspension and vehicle are ignored.

As outlined in Section B.1, the output of the suspension model required by subroutine FCT1 are the total vertical suspension force (TSFV), the total horizontal suspension force (TSFH), total suspension torque about the suspension reference point (TSTORQ), and the vertical accelerations of the unsprung masses ($\ddot{Z}SP(I)$, I = 1,2). (Note that the suspension reference point is defined as the leading axle center.) These quantities may be expressed as:

$$TSFV = SFV(1) + SFV(2) \quad \text{(B-175)}$$

$$TSFH = SFH(1) + SFH(2) \quad \text{(B-176)}$$

$$TSTORQ = TORQ(1) + TORQ(2) + SFV(2) \cdot AA1 \quad \text{(B-177)}$$

where SFV, SFH, and TORQ are defined, respectively, as the total vertical <u>axle</u> force, total horizontal <u>axle</u> force, and the total <u>axle</u> torque about the axle center, and the subscripts (1) and (2)

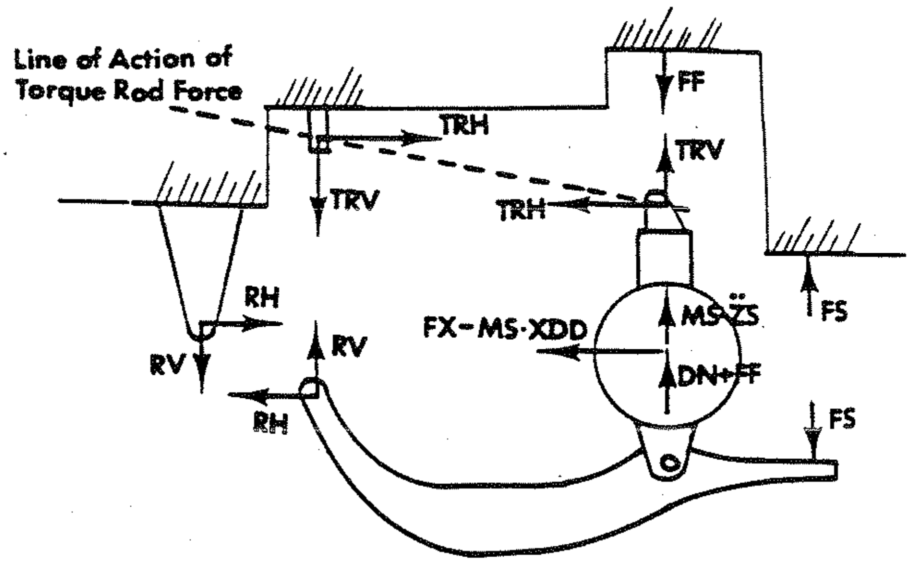

Figure B-30. Dynamic free-body diagram: Axle assembly of the four-bar linkage air suspension.

refer to leading and trailing axles, respectively. In the following analysis, equations for SFV, SFH, and TORQ, as well as $\ddot{Z}SP$, will be developed. Subscripts will be dropped from all notations since the analysis is applicable to either axle.

By definition:

$$SFV \equiv TRV + RV - FS + FF \qquad \text{(B-178)}$$

$$SFH \equiv - TRH - RH \qquad \text{(B-179)}$$

$$TORQ \equiv TRH \cdot AA5 - RV \cdot AA3$$
$$- RH(AA4 - AA3 \cdot \tan AA7A) - FS \cdot (AA2-AA3) \qquad \text{(B-180)}$$

Consider the free body of an entire axle assembly, Figure B-30. Summing moments about the axle center:

$$-TRH \cdot AA5 + RV \cdot AA3 + RH(AA4 - AA3 \cdot \tan AA7A)$$
$$+ FS \cdot (AA2-AA3) + TT = 0 \qquad \text{(B-181)}$$

Then from (B-180) and (B-181)

$$TORQ = -TT \qquad \text{(B-182)}$$

and from the same free body, in the x direction:

$$TRH + RH + FX - MS \cdot XDD = 0 \qquad \text{(B-183)}$$

Combining Equation (B-179) and (B-177)

$$SFH = FX - MS \cdot XDD \qquad \text{(B-184)}$$

Applying Newton's second law to the main suspension arm in the z direction:

$$FS - RV - AV = 0 \qquad \text{(B-185)}$$

and from Equations (B-178) and (B-185)

$$SFV = TRV - AV + FF \tag{B-186}$$

Applying Newton's second law to the axle housing in the z direction:

$$AV - TRV - MS \cdot \ddot{Z}S - DN - FF = 0$$

or (B-187)

$$MS \cdot \ddot{Z}S = AV - TRV - DN - FF$$

and from Equations (B-184) and (B-185)

$$\ddot{Z}S = \frac{-(SFV + DN)}{MS} \tag{B-188}$$

It remains to determine the forces TRV and AV. With these two forces, Equations (B-175) through (B-180), (B-182), (B-184), (B-186), and (B-188) represent the entire solution for the required suspension model output variables.

Summing moments on the torque rod and setting equal to zero leads to

$$TRH = TRV/\tan AA7B \tag{B-189}$$

Summing moments on the axle housing, first about the axle center and then about the main arm pin, and setting equal to zero yields Equations (B-190) and (B-191), respectively.

$$TRH \cdot AA5 + AH \cdot AA4 + TT = 0 \tag{B-190}$$

$$TRH \cdot (AA4+AA5) + (FX - MS \cdot XDD) \cdot AA4 + TT = 0 \tag{B-191}$$

Rearranging (B-190)

$$TRH = \frac{-TT}{AA5} - \frac{AA4}{AA5} AH \qquad (B-192)$$

Substituting (B-189) and (B-192), respectively, into (B-191) and rearranging yields:

$$TRV = -(FX - MS \cdot XDD) \frac{AA4 \cdot \tan AA7B}{AA4 + AA5} - TT \frac{\tan AA7B}{AA4 + AA5} \qquad (B-193)$$

$$AH = (FX - MS \cdot XDD) \frac{AA5}{AA4 + AA5} - \frac{TT}{AA4 + AA5} \qquad (B-194)$$

Now summing moments on the main arm about the body connection pin:

$$FS \cdot AA2 - AV \cdot AA3 + AH \cdot AA3 \cdot \tan AA7A = 0 \qquad (B-195)$$

Substituting (B-194) and (B-195) and solving for AV

$$AV = FS \frac{AA2}{AA3} + [(FX - MS \cdot XDD) \cdot AA5 - TT] \frac{\tan AA7A}{AA4 + AA5} \qquad (B-196)$$

Substituting (B-193) and (B-196) into (B-186)

$$SFV = -FS \frac{AA2}{AA3} - (FX - MS \cdot XDD) \cdot \left(\frac{AA5 \tan AA7A + AA4 \tan AA7B}{AA4 + AA5}\right)$$

$$+ TT \left(\frac{\tan AA7A - \tan AA7B}{AA4 + AA5}\right) + FF \qquad (B-197)$$

In summary, the outputs from the suspension model are

$$\begin{aligned}
&TSFV = SFV(1) + SFV(2) && \text{(a)} \\
&TSFH = SFH(1) + SFH(2) && \text{(b)} \\
&TSTORQ = TORQ(1) + TORQ(2) + AA1 \cdot SFV(2) && \text{(c)} \\
&\ddot{Z}S(1) = \frac{-(SFV(1) + DN(1))}{MS(1)} && \text{(d)} \\
&\ddot{Z}S(2) = \frac{-(SFV(2) + DN(2))}{MS(2)} && \text{(e)}
\end{aligned} \qquad \text{(B-198)}$$

where SFV(I), SFH(I), and TORQ(I) (I = 1,2) may be found from Equations (B-197), (B-184), and (B-182), respectively.

The preceding analysis for a tandem suspension composed of two four-bar linkage-type axles may be easily modified to account for trailing arm linkages (see Figure 2-26) at either or both axles.

Equation (B-198) remains applicable regardless of the linkage arrangement. Further, it can be shown that the equations for SFH and TORQ (Equations (B-184) and (B-182), respectively) remain unchanged for the trailing arm linkage. Thus, to adapt the analysis to the trailing arm arrangement, only the equation for SFV need be altered.

Using the notation from Figure 2-26 and B-31 (free-body diagram of a trailing arm axle), and the definition of SFV:

$$SFV = RV - FS + FF \qquad \text{(B-199)}$$

Equation (B-199) is, of course, identical to Equation (B-178) except for the omission of the vertical torque rod force, TRV.

Summing moments about the axle center in Figure B-31 yields:

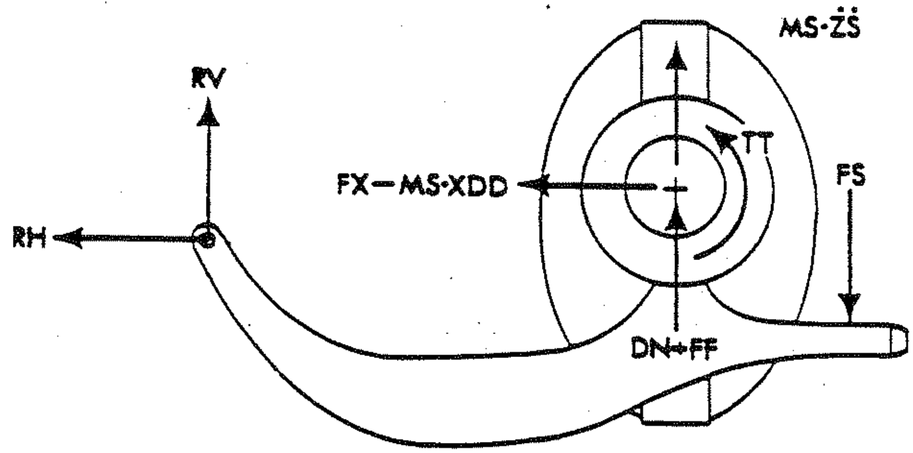

Figure B-31. Dynamic free-body diagram: Trailing arm air suspension.

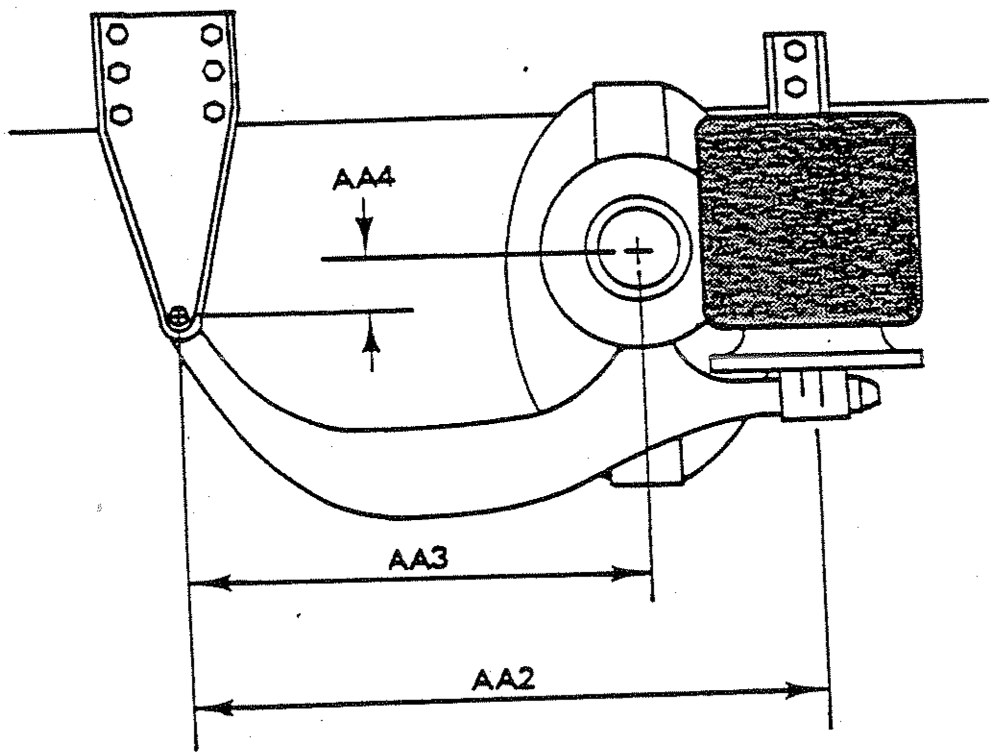

Figure 2.26. The trailing-arm air suspension.

$$RV \cdot AA3 + RH \cdot AA4 + FS(AA2-AA3) - TT = 0 \quad \text{(B-200)}$$

where, from the summation of horizontal forces

$$RH = MS \cdot XDD - FX \quad \text{(B-201)}$$

Combining the three preceding equations

$$SFV = -FS\left(\frac{AA2}{AA3}\right) + \frac{TT + (FX-MS \cdot XDD)AA4}{AA3} + FF \quad \text{(B-202)}$$

Thus, if a trailing arm type axle is to be used, in either leading or trailing position, Equation (B-202) replaces Equation (B-197) as the definition of SFV (i.e., SFV(1) for leading axle or SFV(2) for trailing axle) in Equation (B-198).

Finally, the mechanical linkage analysis can be altered for a single-axle air suspension simply by setting all terms in Equation (B-198) with "(2)" subscripts to zero.

B.9.3 The Air Spring. Basic to the model of the air spring, whose description follows in this section, and to the model of the air delivery system described in Section B.9.4, is the assumption that the behavior of the entire air suspension system can be described as two independent thermodynamic processes. These processes are:

1. A constant mass, reversible polytropic (i.e., PV^n = const) process which is assumed to describe the action of the air in the spring at time (t) over the time period (t) to (t + Δt) where Δt is time step size used in the digital computer program.

2. A constant temperature process assumed to describe the effects of the various air flows in and out of the spring during the time period (t) to ($t + \Delta t$).

For the sake of semantic convention in the following discussions, the first process is attributed to the air spring; the second process is attributed to the air delivery system.

The nomenclature used in the following discussion includes:

h: air spring height

L: air spring load

P: air spring gauge pressure

P_a: air spring absolute pressure

P_{at}: atmospheric pressure

V: air spring internal volume

$(\ )_0$: the subscript 0 refers to the nominal (i.e., operating point) value of the variable. For example, L_0 is the nominal air spring load.

$\Delta(\ )$: the prefix, Δ, refers to a variation from the nominal value. For example, $\Delta L \equiv L - L_0$.

A_L: the effective air spring area with respect to load;

$$A_L \equiv \left.\frac{\partial L}{\partial P}\right|_{h=h_0} \tag{B-203}$$

A_V: effective air spring area with respect to volume;

$$A_V \equiv \left.\frac{dV}{dh}\right|_{h=h_0} \tag{B-204}$$

K_p: air spring constant pressure spring rate;

$$K_p \equiv - \left.\frac{\partial L}{\partial h}\right|_{P=P_0} \tag{B-205}$$

An example of the air spring performance data [19] published by air spring manufacturers appears in Figure B-32. Example values of A_L, A_V, and K_p which derive from this data are given. Upon examining such air spring performance data, it is evident that the following assumptions are reasonable:

$$L = L(P,h) \tag{B-206}$$

and

$$V = V(h) \tag{B-207}$$

(Note the absence of P in Equation (B-207) implies that the internal volume of the air spring is not significantly affected by pressure. This, of course, is not exact.)

In addition, the statements of at least one air spring manufacturer [19] support the assumption of:

$$P_a V^n = C \tag{B-208}$$

where C is a constant, and suggest that

$$n = 1.38 \tag{B-209}$$

This value of n will be assumed here.

If it is further assumed that, within the range of interest about the operating point, linear approximations of Equations (B-206) and (B-207) are sufficiently accurate, then Equations (B-210) and (B-211) are applicable.

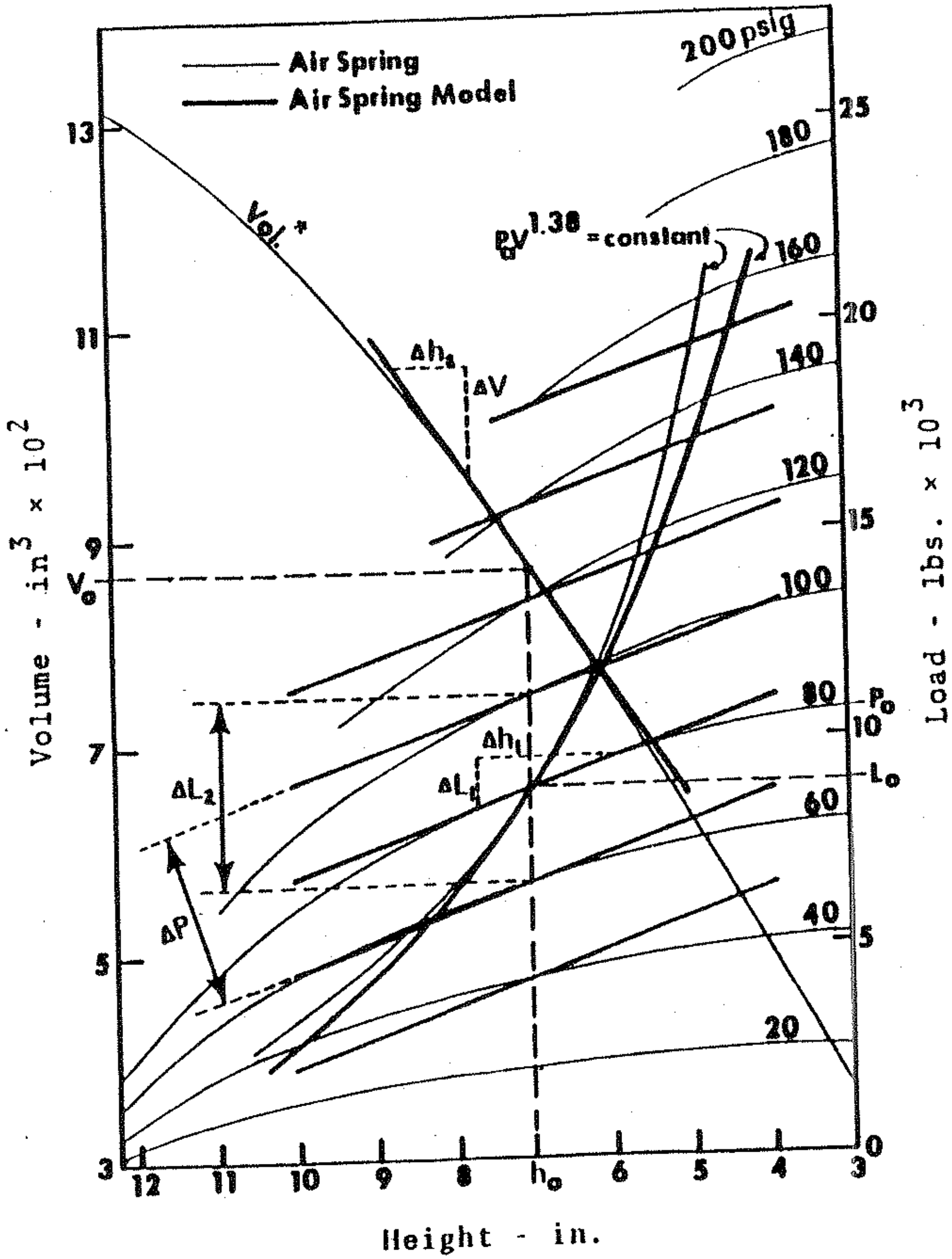

The Operating Point is defined by:

Nominal Volume ; $V_o = 870 \text{ in}^3$

Nominal Height ; $h_o = 7.0 \text{ in}$

Nominal Load ; $L_o = 8800 \text{ lb}$

Nominal Press ; $P_o = 80 \text{ psig}$

The Dynamic Characteristics are:

Effective Area, Volume;

$$A_V \equiv \left.\frac{dV}{dh}\right|_{h_o} = \frac{\Delta V}{\Delta h_2} = 120 \text{ in}^2$$

Effective Area, Load;

$$A_L \equiv \left.\frac{\partial L}{\partial P}\right|_{h_o} \approx \frac{\Delta L_2}{\Delta P} = 112 \text{ in}^2$$

Constant Pressure Spring Rate;

$$K_P \equiv - \left.\frac{\partial L}{\partial h}\right|_{P_o} = - \frac{\Delta L_1}{\Delta h_1} = 667 \frac{\text{lb}}{\text{in}}.$$

*This plot applies to volume vs. height axes
All other plots apply to the load vs. height
only.

Figure B-32. Example Air Spring Data and Model Characteristics

$$\Delta L = \left.\frac{\partial L}{\partial P}\right|_{h=h_0} \cdot \Delta P + \left.\frac{\partial L}{\partial H}\right|_{P=P_0} \cdot \Delta h \qquad \text{(B-210)}$$

$$\Delta V = \left.\frac{dV}{dh}\right|_{h=h_0} \cdot \Delta h \qquad \text{(B-211)}$$

Substituting Equations (B-203) and (B-205) into (B-210) and Equation (B-202) into (B-211) yields:

$$\Delta L = A_L \, \Delta P - K_p \, \Delta h \qquad \text{(B-212)}$$

and

$$\Delta V = A_V \, \Delta h \qquad \text{(B-213)}$$

Substituting nominal values of pressure and volume and a value of 1.38 for n into Equation (B-208):

$$C = (P_0 + P_{at}) V_0^{1.38} \qquad \text{(B-214)}$$

Using this value for C and solving Equation (B-208) for P

$$P = \frac{(P_0 + P_{at}) V_0^{1.38}}{V^{1.38}} - P_{at} \qquad \text{(B-215)}$$

and by the definition of ΔP

$$\Delta P = \frac{(P_0 + P_{at}) V_0^{1.38}}{V^{1.38}} - P_{at} - P_0 \qquad \text{(B-216)}$$

From the definition of ΔV and Equation (B-213)

$$\Delta V = V - V_0 = A_V \cdot \Delta h \qquad (a)$$

(B-217)

or

$$V = V_0 + A_V \cdot \Delta h \qquad (b)$$

Substituting Equation (B-217b) into (B-215) yields:

$$\Delta P = \frac{(P_0 + P_{at})V_0^{1.38}}{[V_0 + A_V \cdot \Delta h]^{1.38}} - P_{at} - P_0 \qquad \text{(B-218)}$$

Equations (B-212), (B-213), and (B-218) constitute a mathematical representation of the proposed air spring model. The input to the model is Δh, the change in air spring height, and the output is ΔL, the change in air spring vertical force. A graphical representation of this model appears in Figure B-32. Figure B-32 gives an example of the air spring model performance characteristics of an example air spring.*

In the figure, the lines of constant pressure and the plot marked "Vol." represent published data. The various straight lines are the model's approximation of this data according to the values of A_V, A_L, and K_p obtained for the arbitrarily chosen operating point. The two plots marked "$P_a V^{1.38}$ = Constant" are the results of applying the empirical data and the model characteristics, respectively, to this equation (i.e., each of these plots represents a solution to the simultaneous equations:

$$V = V(h) \qquad (a)$$

$$P_a V^{1.38} = \text{Constant} \qquad (b) \qquad \text{(B-219)}$$

$$L = L(P,h) \qquad (c)$$

---

*Firestone Airide ®, No. 21. [19].

The lighter plot results when Equations (a) and (c) are solved using actual air spring data; the darker line comes from employing the air spring model to solve Equations (a) and (c).

Note that in Figure B-32, the values of A_V, A_L, and K_p were determined by designating the operating point to be identical to the static condition. In certain situations, improved model behavior may be obtained by a slight variation of this procedure. For example, consider the case when this spring is being used on the rear of a straight truck being studied under braking only. Assuming that the operating point represents the static loading condition, it would generally be expected that loads on the spring would always be less than or equal to the nominal load and spring height would be greater or equal to nominal height. Consequently, the model would operate only to the left of and below the operating point. By choosing A_V to more nearly represent the slope of the "Vol." plot in this region, significant improvement in model performance in the same region can be gained. (See Figure B-33.)

Similar adjustment of A_L to more nearly represent the vertical spacing of the constant pressure lines in the region of interest will also improve performance. For the example spring considered here, K_p appears to be near optimum as shown. In general, the goal when choosing the values of A_V, A_L, and K_p is to obtain the most accurate linear approximations of the spring data (both "Vol." and constant pressure plots) as possible within the expected region of operation.

B.9.4 <u>The Air Delivery System</u>. The discussion of the previous section assumed no air flow into or out of the air spring. This, of course, is not the case. Figure B-34 diagrams the plumbing system of a typical tandem air suspension.* As

*Note that height regulating valves are indicated since this model is intended for use as a full suspension, not as tag axles.

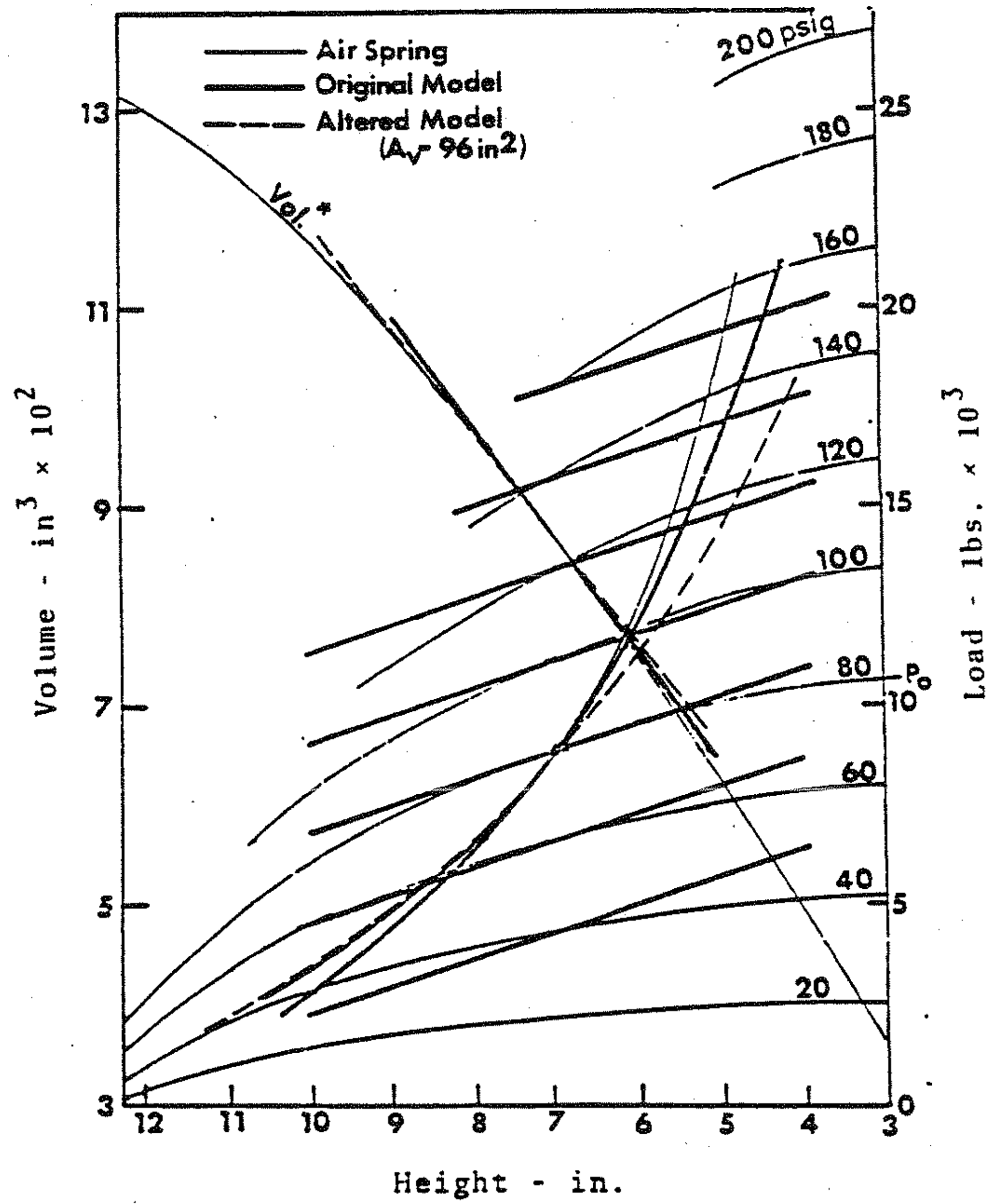

Figure B-33. Improved model performance within a limited operating range.

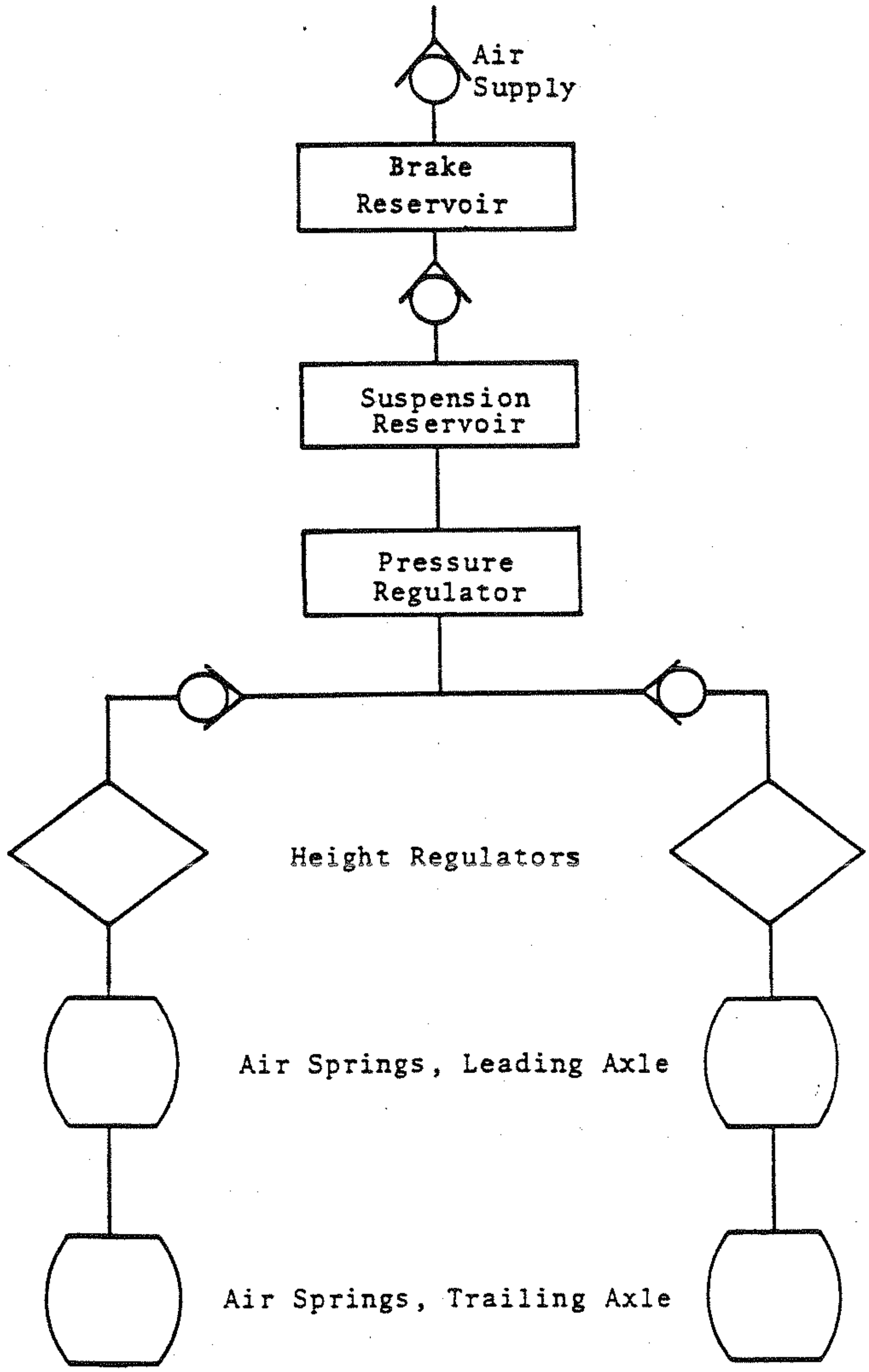

Figure B-34. Air Suspension Plumbing Diagram shown, air may enter or exit an air spring via the height regulator or through its interconnections with the other spring on the same side of the vehicle.

Air flow through the height regulators is typically quite slow, but may have an effect on the pitch attitude of the vehicle near the end of a high-speed stop. More importantly, the interconnection between the two axles of a tandem may have a significant load leveling effect.

The same model is proposed for each of the several flow paths (to be enumerated later). Basic to this model are the assumptions that (1) during a single time step ($\Delta t = 0.0025$ sec) temperature in the air spring is constant, and (2) the mass flow of air in a given flow path may be described by:

$$\left(\frac{dM}{dt}\right)_i = C_i' \left(P_{e_i} - P\right) \qquad \text{(B-220)}$$

where

$\left(\frac{dM}{dt}\right)_i$: the mass rate of air flow into (positive) the spring via the particular flow path

P: the gauge air pressure in the spring

P_{e_i}: the gauge air pressure at the opposite end of flow path i (supply pressure, atmospheric pressure, or pressure in the other spring)

C_i': a constant property of the flow path i.

Then for either air spring, assuming the ideal gas law

$$(P + P_{at}) \cdot V = M \cdot R \cdot T \qquad \text{(B-221)}$$

where

P_{at} is atmospheric pressure

R is the gas constant

V is the air spring volume

T is the absolute temperature in the spring

M is the air mass in the air spring.

Then by differentiating

$$\frac{dM}{dt} = \frac{d}{dt}\left[\frac{(P + P_{at})V}{R \cdot T}\right] = \sum_{i=1}^{n} \left(\frac{dM}{dt}\right)_i \qquad \text{(B-222)}$$

where n is the number of flow paths.

Since R and T are constants, Equation (B-222) may be written

$$\sum_{i=1}^{n} \left(\frac{dM}{dt}\right)_i = \frac{1}{R \cdot T}\left[(P + P_{at})\frac{dV}{dt} + V\frac{dP}{dt}\right] \qquad \text{(B-223)}$$

Combining Equations (B-220) and (B-223) and rearranging:

$$\frac{dP}{dt} = \frac{1}{V}\left[\sum_{i=1}^{n} C_i(P_{e_i} - P) - (P + P_{at})\frac{dV}{dt}\right] \qquad \text{(B-224)}$$

where

$$C_i = C_i' \cdot R \cdot T \qquad \text{(B-225)}$$

The time step at which the HSRI simulation program proceeds ($\Delta t = 0.0025$ sec) is extremely small relative to the expected dynamic behavior of the air delivery system. Consequently, the simplest form of digital integration will be adequate for the solution of Equation (B-224). Therefore, from Equation (B-224)

$$\Delta P_D = \frac{1}{V_{AV}} \left[\sum_{i=1}^{n} C_i(P_{e_i} - P_{AV}) - (P_{AV} + P_{at}) \left(\frac{dV}{dt}\right)_{AV} \right] \Delta t \qquad \text{(B-226)}$$

where the subscript (AV) indicates an average value over the time step and the subscript (D) indicates "of the delivery system."

Determination of the values of V_{AV}, P_{AV}, and $\left(\frac{dV}{dt}\right)_{AV}$ to be substituted into the right-hand side of Equation (B-226) will be discussed in Section B.9.5. Suffice to say they will be approximations to their average values over the time step.

Figure B-28 illustrates all the flow paths available in the tandem air suspension model. As shown in the figure, there is an input and exhaust coefficient plus a switching mechanism associated with the air spring of each axle. Either of these regulators may be removed from the model by setting the appropriate flow coefficients to zero. A flow coefficient is also available to describe flow between the axles. Associated with each switching mechanism is a time lag as described in Section 2.1.8.

The details of the interrelationship between the air spring and air delivery system models will be covered in the following section. In general, the value of ΔP_D determined by this air delivery model will be used as a modifier to the value of ΔP associated with the air spring model. (See Equation (B-217).)

B.9.5 <u>The Complete Model</u>. In this section, the interrelationships between the three portions of the air suspension model will be described. A conceptual flow diagram of the model appears in Figure B-35. It may be helpful in understanding the material in this section to refer to this figure. Initially, the air spring and air delivery system models will be combined to form a total air system model. To complete the model, air and mechanical systems will then be combined.

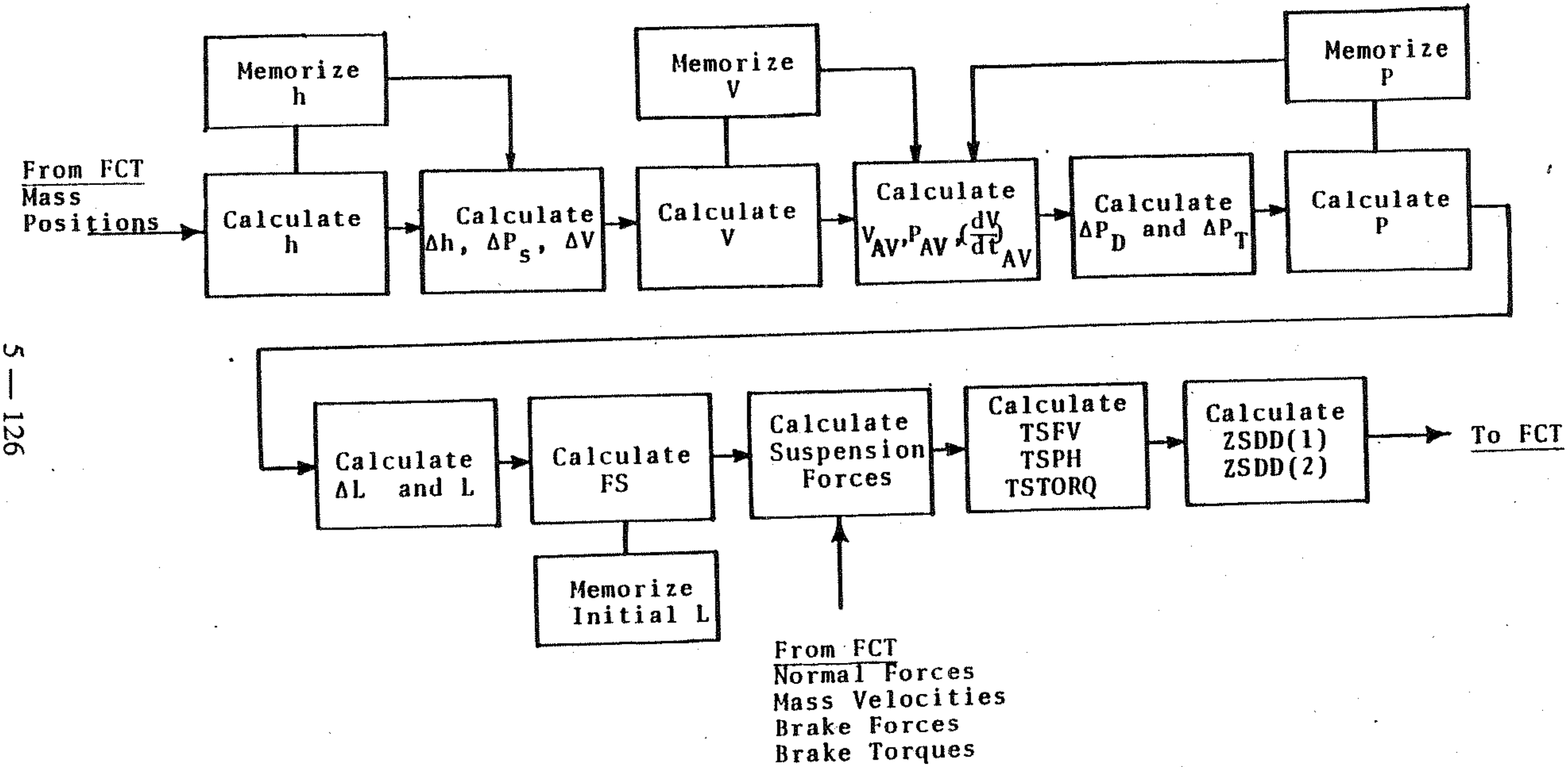

Figure B-35. Air Suspension Model Flow Diagram

To this point, the air system has been considered as two separate systems, the air spring and the air delivery system. Important to the interaction of these systems is the fact that, in general terms, the dynamic response of the air delivery system can be expected to be very much slower than that of the air spring-tire spring-unsprung mass system. (Indeed, it is this difference in response which has allowed the separation of the spring and delivery system.) Since this is the case, it can be expected that over the short time span of a single integration time step, the total change in air pressure in the air spring (ΔP_T) will be dominated by the effect of the air spring as indicated by Equation (B-217). (ΔP as calculated from Equation (B-217) will be designated ΔP_S, i.e., ΔP of the spring model, in this section.) By comparison, ΔP_D, the change in pressure due to the delivery system, will be small for any given time step. The more important effect of ΔP_D will be its accumulative effect over a longer period of time.

Now defining,

P_t: air spring pressure at the beginning of a time step

P_{AV}: average air spring pressure during the time step.

Then assuming the total air spring pressure change may be written

$$\Delta P_T = \Delta P_S + \Delta P_D \qquad \text{(B-227)}$$

it follows that

$$P_{AV} = P_t + \Delta P_T/2 = P_t + \frac{\Delta P_S + \Delta P_D}{2} \qquad \text{(B-228)}$$

But from the preceding discussion

$$\Delta P_D \ll \Delta P_S \tag{B-229}$$

and therefore it may be assumed

$$P_{AV} = P_T + \Delta P_S/2 \tag{B-230}$$

The average pressure, P_{AV}, of Equation (B-23) is then the value to be used in the right-hand side of Equation (B-226) to calculate ΔP_D.

In addition to P_{AV}, the right-hand side of Equation (B-226) also requires values of V_{AV} and $(dV/dt)_{AV}$. These values become available simply by performing the digital integration to determine the new positions of the sprung and unsprung masses (via HPCG) before solving Equation (B-226). With this done, the mass positions, and consequently the spring heights, are known both at the beginning and end of the particular time step. Then, Δh is also known for that time step, and from Equation (B-213) ΔV is known. By definition

$$(dV/dt)_{AV} = \Delta V/\Delta t \tag{B-231}$$

and

$$V_{AV} = V_t + \Delta V/2 \tag{B-232}$$

where V_t is the volume at the beginning of the time step.

At this point, sufficient information is available to calculate the total pressure change, ΔP_T, which, with Δh, is substituted into Equation (B-212) (replace ΔP with ΔP_T) to obtain the change in spring force, ΔL. Note that Equation (B-212) was derived independently of the assumed equation of operation ($P_a V^{1.38}$ = Const.) and is valid regardless of the source of ΔP or Δh.

The final step in the operation of the air system model is an adjustment of the "constant" in the equation.

$$P_a V^{1.38} = \text{constant} \tag{B-233}$$

Combining Equation (B-233) and (B-214) yields

$$P_a V^{1.38} = (P_0 + P_{at}) V_0^{1.38} \tag{B-234}$$

Note that the basic assumptions, given in the opening remarks of Section B.9.3, states that Equation (B-234) holds over a single integration time step. However, due to the action of the air delivery system, P_0 and V_0 must be updated between integration steps. As the solution according to the model progresses through a time step, ΔP_S is first found according to an equation derived from Equation (B-233). Next, this pressure change is altered by the amount, ΔP_D, and, thus, is no longer compatible with Equation (B-233). Consequently, to prepare the model for solution in the next time step the values of P_0 and V_0 must be updated. That is,

$$P_{0_{t+\Delta t}} = P_{0_t} + \Delta P_T \quad \text{(a)}$$

(B-235)

$$V_{0_{t+\Delta t}} = V_{0_t} + \Delta V \quad \text{(b)}$$

A more graphical representation of this operation appears in Figure B-36. The initial condition of the air spring model is represented by points A and A'. The value Δh is determined by (1) integration of the dynamic variables to obtain ZSP and (2) the geometry of the mechanical linkage. ΔP_S is determined by following the "operating line" ($P_a V^{1.38} = C_1$) to point B

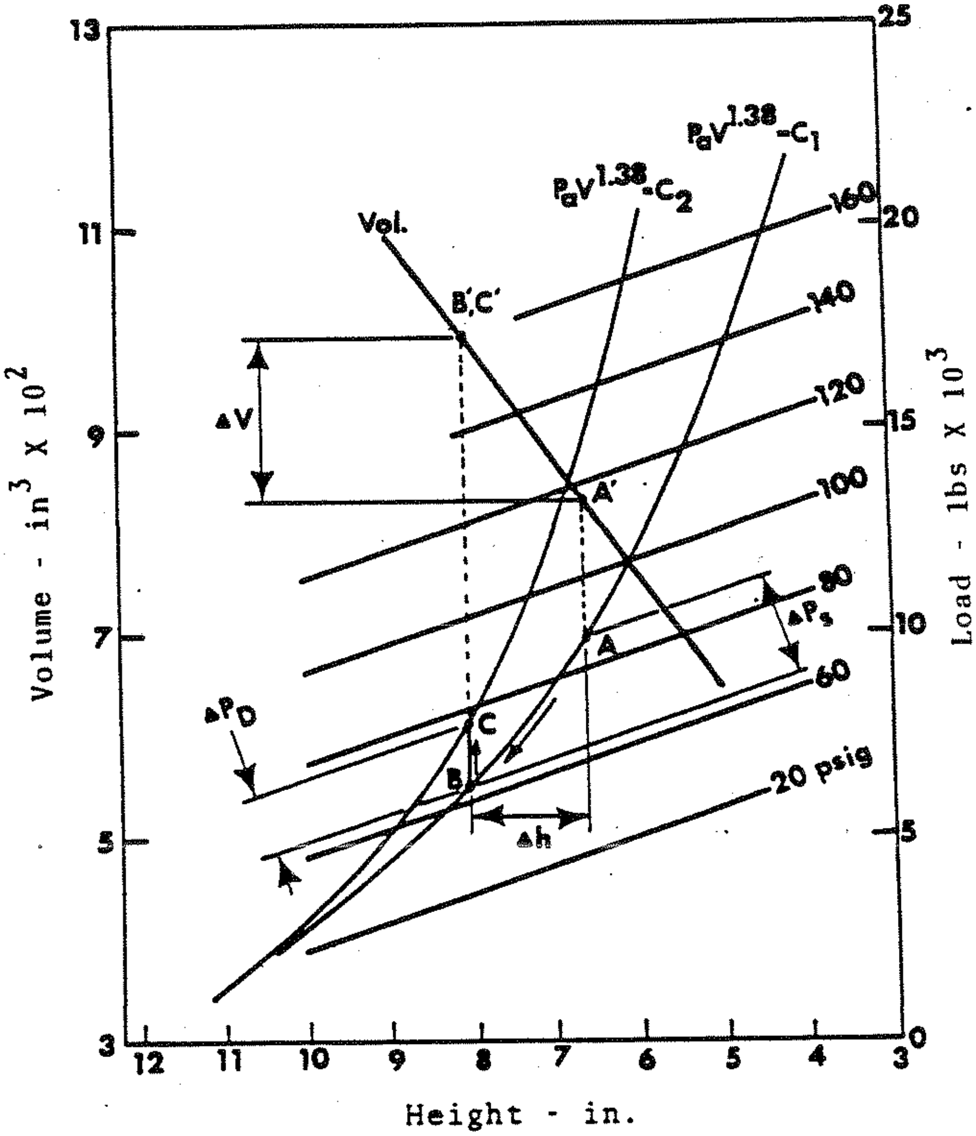

Figure B-36. Air Suspension Operation Over a Single Time Step while ΔV is determined by following the "Vol." line to B'. ΔP_D is then calculated and the final condition of the air spring is determined by moving from point B to point C, a distance of ΔP_D along a line of constant h. (Constant h because it can change no more than Δh.) The condition of the air spring no longer agrees with the original operating line. Consequently, the values of P_0 and V_0 are updated to pressure and volume of points C and C', respectively (h_0 and L_0 are similarly updated), and a new operating line is established according to

$$P_a V^{1.38} = C_2 \qquad \text{(B-236)}$$

where

$$C_2 = (P_0 + P_{at}) V_0^{1.38} \qquad \text{(B-237)}$$

using the updated values of P_0 and V_0.

This completes the operation of the air system model. It remains only to relate the air spring load, L, and height, h, to the mechanical linkage model. Designating h_i and L_i as the initial (static) values of h and L, then from the geometry and notation of Figure B-28

$$h - h_i = AA2/AA3\ ZSP \qquad \text{(B-238)}$$

and

$$FS = L - L_i \qquad \text{(B-239)}$$

Equations (B-238) and (B-239) complete the proposed model of the air suspension system. Equation (B-238) is used to compute Δh for input to the air system model. Equation (B-239) is used to compute the dynamic spring force needed by FCT to compute the derivatives for the next integration step.

B.9.6 <u>Static Considerations</u>. The preceding sections have described the various portions of the dynamic air suspension model. It remains to describe the calculations which determine the static normal tire loads, air spring load and air spring pressure.

Using the definitions given in Section B.1 and rigid body analysis, applied to the static free-body diagram of Figure B-37, it can be shown that

$$STORQ = SRATIO \cdot SSFV + SCONST \qquad (B\text{-}240)$$

$$SSFV = WS1 + WS2 - NS1 - NS2 \qquad (B\text{-}241)$$

$$STORQ = (WS2-NS2)AA1 \qquad (B\text{-}242)$$

where WS1 and WS2 are the leading and trailing unsprung weights, respectively, and NS1 and NS2 are the static normal tire loads at the leading and trailing axles, respectively. Combining these three equations leads to:

$$NS1 = WS1 + SSFV \left[\frac{SRATIO}{AA1} - 1\right] + \frac{SCONST}{AA1} \qquad (B\text{-}243)$$

$$NS2 = WS1 + WS2 - NS1 - SSFV \qquad (B\text{-}244)$$

The values of SRATIO and SCONST are determined in two different ways, depending on whether the tandem axles are independent or dependent. If an air line interconnection exists between the air springs of the two axles (i.e., the input parameter CINTR is non-zero), the axles are "dependent" by virtue of the fact that the static air spring pressure at the two axles is identical. In this case, it can be shown that

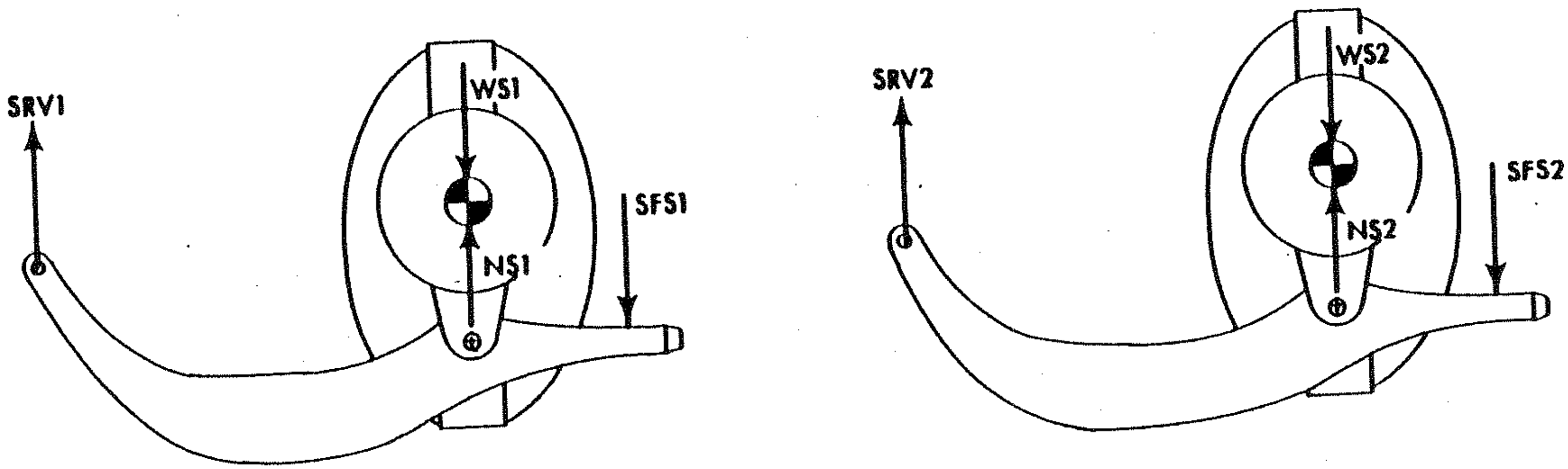

Figure B-37. Static Free-Body Diagram:
The Air Suspension.

$$SRATIO = A_{L1} \cdot AA2(1)/AA3(1) + A_{L2} \cdot AA2(2)/AA3(2) \qquad \text{(B-245)}$$

and

$$SCONST = (L_{01} \cdot AA2(1)/AA3(1) + L_{02} \cdot AA2(2)/AA3(2)$$

$$\cdot\ SRATIO - L_{02} \cdot AA1 \cdot AA2(2)/AA3(2) \qquad \text{(B-246)}$$

If the tandem axles are independent (CINTR = 0), then the static condition of the axles is indeterminate. In this case, the user must input the parameter, PRCTN1, which is the percentage of total tire normal load carried at the leading axle. In this case, it can be shown that

$$SRATIO = AA1(100\text{-}PRCTN1)/100 \qquad \text{(B-247)}$$

$$SCONST = -SRATIO \cdot WS2 - \frac{PRCTN1}{100\text{-}PRCTN1}(WS1+WS2) \qquad \text{(B-248)}$$

For either leading or trailing axles, the static air spring load (SFS) and pressure (SP) can be shown to be

$$SFS = (NS - WS)\,\frac{AA3}{AA2} \qquad \text{(B-249)}$$

$$SP = \frac{SL - L_0}{A_L} + P_0 \qquad \text{(B-250)}$$

where the "1" and "2" designations have been dropped since these equations are applicable to either axle.